Knowledge-Based Systems 225 (2021) 107117

Contents lists available at ScienceDirect

Knowledge-Based Systems

journal homepage: www.elsevier.com/locate/knosys

A robust elastic net via bootstrap method under sampling uncertainty for significance analysis of high-dimensional design problems

Hansu Kim, Tae Hee Lee *

Department of Automotive Engineering, College of Engineering, Hanyang University, Seoul 04763, Republic of Korea

ARTICLE INFO

Article history:
Received 11 January 2021
Received in revised form 19 March 2021
Accepted 30 April 2021
Available online 3 May 2021

Keywords:
Significance analysis
Elastic net
Sampling uncertainty
Bootstrap method
Statistical criterion
Significance measure

ABSTRACT

The elastic net can analyze the significance of input variables regardless of the data type of input variables and statistical assumptions. However, the significance can alter owing to sampling uncertainty arising from the design of experiments such as the optimal Latin hypercube design which may generate different datasets at each time even if the same number of data points is sampled. This sampling uncertainty affects elastic net modeling and causes incorrect inferences. Additionally, studies on the reduction of sampling uncertainty for the elastic net are not addressed yet. Therefore, this study proposes a robust elastic net via bootstrap method (RENBOOT) to reduce sampling uncertainty. Relevance of input variables was analyzed using the statistical criterion that is based on bootstrap confidence intervals for estimated coefficients of the elastic net to accurately analyze the significance of input variables. Then, the significance of relevant input variables was analyzed using the significance measure that is based on bootstrap replications for the estimated coefficients of the elastic net. Through mathematical examples, the accuracies (balanced accuracy, F1 score, Cohen's kappa, root mean square error) of the relevance and significance of input variables using RENBOOT were verified to be highly improved compared with those of the elastic net. Furthermore, the significance of input variables for the body-in-white of a vehicle was analyzed using RENBOOT, which can give useful information for significant input variable selection. That is, we expect that design optimization can be performed efficiently by selecting significant input variables based on the significance via RENBOOT.

© 2021 Elsevier B.V. All rights reserved.

1. Introduction

High-dimensional, computationally expensive, black-box problems pose several challenges in design optimization [1]. Such problems are known as the curse-of-dimensionality [2], size of problem [3], and so on. As the number of input variables increases, optimization costs increase owing to the expansion of the design space. Computationally expensive black-box (EB) problems arise from complex simulation analyses such as computational fluid dynamics, dynamics analyses, and finite element analyses. Although the EB problem is one of the major challenges in optimization, several surrogate-model-based methods have also been studied to solve this problem [4–13]. However, dealing with high-dimensional problems remains a challenge.

Methods such as variable selection and variable screening have been used to solve the high-dimensional problem [14–18]. These methods reduce the number of input variables by removing irrelevant input variables and selecting significant input variables for the responses. To remove irrelevant input variables and select the significant input variables, the significance of input variables must be analyzed. Significance is the influence of input variables on a response within a design domain and can be obtained by calculating the percentage contribution ratio [19] based on the analysis of variance (ANOVA) [20]. However, ANOVA assumes that the data type of input variables is categorical, and the normality, homogeneity of variance, and independence of observations must be satisfied.

To avoid these assumptions, this study introduces the elastic net [21], which is one of the widely used feature selection methods in data mining. Significance is analyzed based on the coefficients of the elastic net. Generally, given datasets are used to build the elastic net in computer science fields. On the other hand, in the design optimization of a computational model, datasets are generally not given, so data points are sampled using the design of experiments (DOE). The data points for the computational model are used for the significance analysis, surrogate modeling, reliability analysis, and so on. In the case of the DOE such as the optimal Latin hypercube design (OLHD) [22] and maximin distance design [23], different datasets can be sampled at each time, as depicted in Fig. 1. In other words, the coefficients of

* Correspondence to: Department of Automotive Engineering, College of Engineering, Hanyang University, 222 Wangsimni-ro, Seongdong-gu, Seoul 04763, Republic of Korea.
E-mail address: thlee@hanyang.ac.kr (T.H. Lee).

https://doi.org/10.1016/j.knosys.2021.107117
0950-7051/© 2021 Elsevier B.V. All rights reserved.

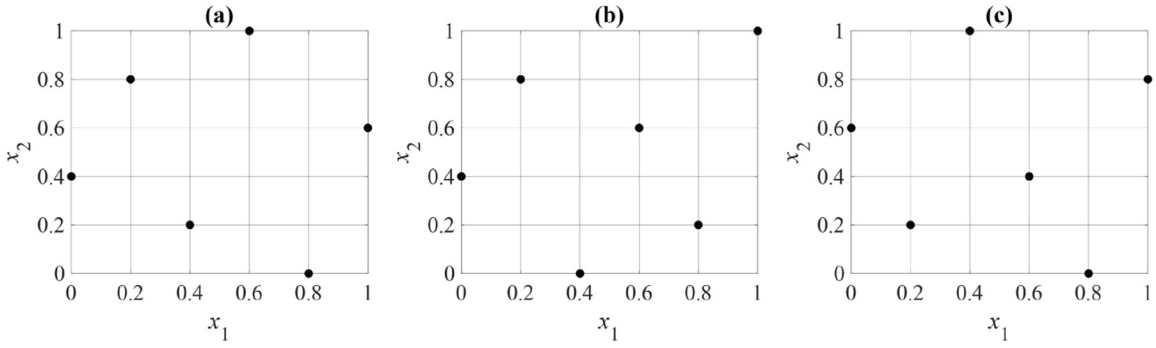

Fig. 1. Sampling uncertainty for 2D design space data sampled using OLHD.

the elastic net can differ based on the sampling uncertainty, resulting in different significance values depending on the datasets. Additionally, when the number of input variables increases, the sampling uncertainty tends to increase. Certainly, when the given datasets exist, it is no need to sample data points, so there will be no sampling uncertainty. However, if significance analysis is performed using the elastic net for the design optimization of a computational model, the sampling uncertainty leads to incorrect inferences (relevance and significance of input variables).

Recently, a rough entropy-based uncertainty measure was used to evaluate the roughness and accuracy of knowledge [24]. The proposed method afforded better computational efficiency than heuristic feature selection algorithms in incomplete decision systems. A weighted elastic net (WEN) was proposed [25] to reduce the dimensionality of face recognition. WEN is strictly convex, which guarantees the grouping effect by solving the problem of classical sparse representation. An adaptive WEN support vector machine (AWENSVM) was proposed [26] to improve its performance in imbalanced data classification problems. AWENSVM exhibited better performance and is more robust than the standard SVM and other existing weighted SVMs. A robust and cost-effective feature selection method [27] was proposed to deal with the ambiguity and uncertainty of the feature cost. The proposed method extended the ℓ_1-norm SVM by incorporating a budget constraint to preserve classification accuracy with the least expensive features. However, none of these studies considered the sampling uncertainty of the elastic net.

Some studies have dealt with sampling uncertainty directly [28] and indirectly [29,30]. Klau et al. focused on the issue of sampling uncertainty in omics biomarker selection. Although they proposed a general resampling-based framework to quantify sampling uncertainty, they did not suggest a method to reduce it. Gorostiaga and Rojo-Álvarez [29] and Muñoz-Romero et al. [30] introduced bootstrap resampling to robustly estimate statistical descriptions of the input feature relevance and importance (significance). In particular, Gorostiaga and Rojo-Álvarez proposed a statistical criterion that analyzed the relevance of input features. Muñoz-Romero et al. proposed an importance measure that analyzed the importance of input features. However, the objective of these two studies was classification-model-based feature selection; in other words, the response should have discrete values such as $\{-1, +1\}$ or $\{0, +1\}$. However, in design optimization, as the response is continuous, classification-model-based feature selection methods cannot be used to analyze significance. Furthermore, because these two studies attempted to reduce the noise in data, the source of uncertainty was different from the sampling uncertainty considered in this study. To the best of our knowledge, sampling uncertainty reduction for the elastic net has not been addressed in previous studies thus far.

Therefore, this study proposes a robust elastic net via the bootstrap method (RENBOOT) to reduce sampling uncertainty. The bootstrap method [31], which is a widely used resampling method, was employed. The relevance of input variables was analyzed using the statistical criterion [29] that is based on the bootstrap confidence intervals (BCIs) for the estimated coefficients of the elastic net. That is, in order to accurately analyze the significance of input variables, the screening of irrelevant input variables is preceded using the statistical criterion. Additionally, a significance measure based on bootstrap replications for the estimated coefficients of the elastic net was used to analyze significance. Through mathematical examples, the accuracies of the relevance and significance of input variables using RENBOOT were demonstrated to be higher than those of the elastic net. Furthermore, RENBOOT was applied to the body-in-white (BIW) of a vehicle [32]. The significance obtained using RENBOOT was demonstrated to be reasonable in terms of physical relationships.

The remainder of this article is organized as follows. In Section 2, the preliminaries of RENBOOT, namely the elastic net and bootstrap method, are described. In Section 3, RENBOOT is proposed, and the statistical criterion and significance measure are described. Additionally, the description of the mathematical examples, accuracy measures, and comparison of results are presented in detail. In Section 4, the input variables and responses of the engineering problem and the results of RENBOOT are discussed. Finally, the conclusions of this study are summarized in Section 5.

2. Preliminaries

2.1. Elastic net

In machine learning, the bias–variance trade-off is a crucial problem (see Fig. 2). As the ridge has low bias and high variance for the prediction error, it can lead to overfitting. In contrast to the ridge, lasso has high bias and low variance for the prediction error, which can lead to underfitting. Generally, the underfitting problem can be solved by increasing the model complexity. However, when the model complexity increases significantly, the overfitting problem arises. The elastic net was developed to balance the bias and variance for the prediction error and improve some limitations of lasso. The elastic net achieves the optimum model complexity by minimizing the total prediction error.

The elastic net was developed based on the linear regression model as follows:

$$\hat{\mathbf{y}} = \hat{\beta}_0 + \mathbf{x}_1\hat{\beta}_1 + \cdots + \mathbf{x}_n\hat{\beta}_n \tag{1}$$

where n is the number of input variables, $\mathbf{x}_i$ is the ith input variable vector, $\hat{\mathbf{y}}$ is a predicted response vector, and $\hat{\beta}_i$ is the ith predicted coefficient. The coefficients are estimated using the following optimization problem:

$$\hat{\boldsymbol{\beta}} = \arg\min_{\boldsymbol{\beta}} \left[\frac{1}{2N} \left(\mathbf{y} - \mathbf{X}^{\mathrm{T}}\boldsymbol{\beta}\right)^2 + \lambda \sum_{i=1}^{n} \left\{ \frac{1}{2}\left(1-\alpha\right)\beta_i^2 + \alpha\left|\beta_i\right| \right\} \right]$$

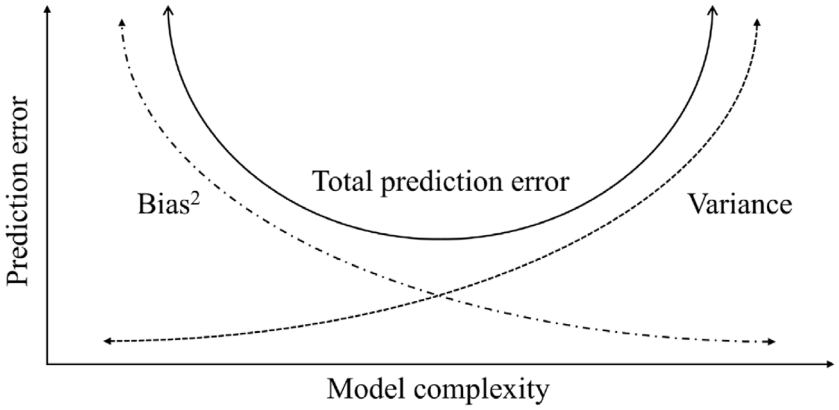

Fig. 2. Bias–variance trade-off of machine learning model.

(2)

where N is the number of data points, $\mathbf{X}$ is an input variable matrix, $\mathbf{y}$ is a response vector, α is a parameter, and λ is a penalty parameter. In Eq. (2), the first term and second terms are the residual sum of squares and elastic net penalty, respectively. When λ increases, the estimated coefficients with a value of zero increase. In other words, the weight of the input variable screening is greater than that of increasing the prediction accuracy of the elastic net. Because it is necessary to ensure the balance between the prediction accuracy and input variable screening, λ is determined using leave-one-out cross validation. In addition, α has a range greater than 0 and less than 1. The closer of α is to 0, the closer the estimated coefficients are to those estimated by the ridge. When the weight for the ℓ_2-norm term increases, the number of input variables whose coefficients are exactly 0 decreases. In contrast, the closer the value of α is to 1, the closer the estimated coefficients are to those estimated by lasso. When the weight for the ℓ_1-norm term increases, the number of input variables whose coefficients are exactly 0 increases. In this study, $\alpha = 0.5$ was used, which is the center of the range. In addition, $\mathbf{X}$ and $\mathbf{y}$ are normalized to have values from 0 to 1 and -1 to 1, respectively.

The relevance of input variables is analyzed based on the estimated coefficients. In other words, an input variable x_i is relevant to a response y if $\hat{\beta}_i$ is a nonzero value. Otherwise, x_i is an irrelevant input variable. For example, when the coefficients are estimated, as depicted in Fig. 3(a), x_1, x_2, and x_4 are relevant input variables and x_3 is an irrelevant input variable. Furthermore, the significance of input variables is analyzed based on the magnitudes of the estimated coefficients. In the case of Fig. 3(a), the ranking of the significances of input variables is x_1, x_4, and x_2. However, the estimated coefficients can differ owing to sampling uncertainty, as in Fig. 3(b) and (c). In the case of Fig. 3(b), the ranking of the significances is x_4, x_1, and x_2. In the case of Fig. 3(c), x_3 is analyzed as a relevant input variable, which is not the same as Fig. 3(a) and (b). Because different inferences can be made, as depicted in Fig. 3, it is necessary to reduce sampling uncertainty.

2.2. Bootstrap method

The BCIs for the estimated coefficients are calculated using bootstrap replications for the estimated coefficients through bootstrap resampling. The ordinary bootstrap resampling method is widely used. This method samples a significantly large number B of bootstrap datasets with replacement for N original data points, as depicted in Fig. 4, where the superscript "*" indicates bootstrap replications. Generally, the number of data points for each bootstrap dataset is resampled as N to be the same as the number of the original dataset. The numbers of bootstrap replications, B, used are as 500, 1000, 2000, 5000, and 10 000, and it is known that a parameter can be accurately estimated as B increases. Because the computational costs increase in proportion to B, it is necessary to use an appropriate value of B considering computer performance and available time. In this study, $B = 1000$ was used.

From the point of view of the total bootstrap datasets, specific data points can be sampled mostly because of random sampling characteristics, that is, the frequencies of the data points may not be equal to one another. Balanced bootstrap resampling [33] was developed to address this problem. Using balanced bootstrap resampling, each data point appears exactly B times. Balanced bootstrap resampling concatenates B copies of the original dataset and randomly permutes $B * N$ data points. Next, the $B * N$ data points are split by N data points B times. Thus, this study used the balanced bootstrap resampling method to accurately obtain the BCIs for the estimated coefficients.

The BCIs are calculated using the basic, bootstrap-t, percentile, and bias-corrected and accelerated (BCa) methods [31,34]. The basic and bootstrap-t methods, which are a pivotal family, are not transformation respecting. Additionally, the bootstrap-t method requires the estimation of the standard deviation of the estimated parameter. The percentile and BCa methods, which are a non-pivotal family, can estimate the confidence intervals without restrictions. The percentile method is straightforward and widely used (see Fig. 5). However, when the bootstrap distribution of the estimated parameter is not nearly symmetric, errors in the BCIs can be substantial. The BCa method [35] was developed to address this problem.

The BCa method calculates BCIs by considering the lack of symmetry, shape, and skewness of the bootstrap distribution. It calculates the BCIs with confidence level α as follows:

$$\begin{aligned} &\mathrm{CI}^*_{\hat{\beta}}\text{: } \left[\hat{\beta}^{*,\mathrm{LB}},\ \hat{\beta}^{*,\mathrm{UB}}\right] = \left[\hat{\beta}^{*(\alpha_1)}, \hat{\beta}^{*(\alpha_2)}\right] \\ &\alpha_1 = \Phi\left(\hat{z}_0 + \frac{\hat{z}_0 + z^{(\alpha/2)}}{1 - \hat{a}\left(\hat{z}_0 + z^{(\alpha/2)}\right)}\right) \\ &\alpha_2 = \Phi\left(\hat{z}_0 + \frac{\hat{z}_0 + z^{(1-\alpha/2)}}{1 - \hat{a}\left(\hat{z}_0 + z^{(1-\alpha/2)}\right)}\right) \end{aligned} \tag{3}$$

where $\hat{a}$ is an estimate of the acceleration constant a; $z^{(\alpha)} = \Phi^{-1}(\alpha)$ is the 100αth percentile point of the standard normal distribution; $\hat{z}_0$ is an estimate of bias-correction constant z_0; $\hat{\beta}^{*(\alpha)}$ is the 100αth percentile of B bootstrap replications for $\hat{\beta}$; $\hat{\beta}^{*,\mathrm{LB}}$ and $\hat{\beta}^{*,\mathrm{UB}}$ are, respectively, the lower and upper bounds of the BCIs for $\hat{\beta}$; and Φ is the standard normal cumulative distribution

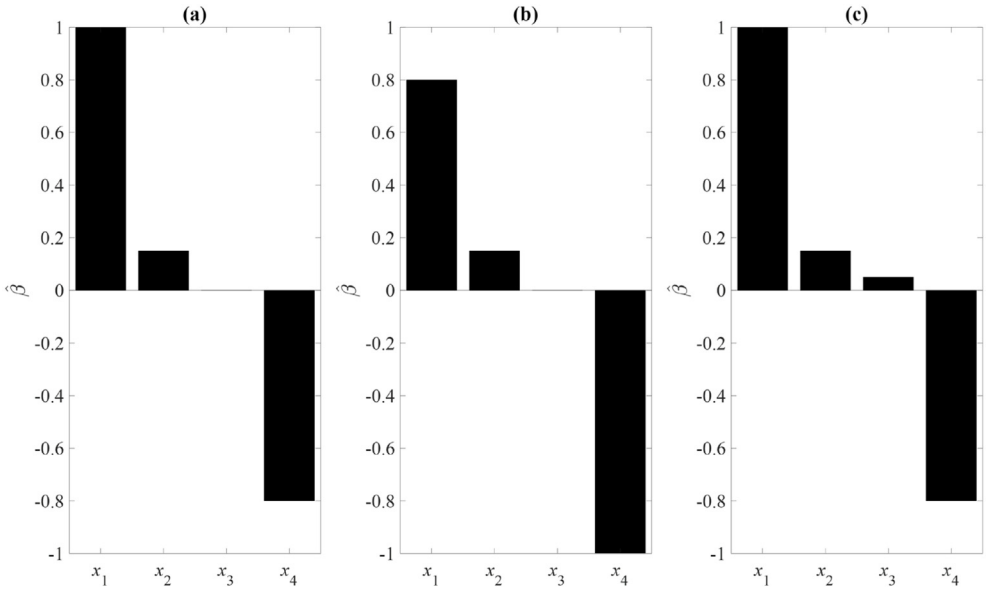

Fig. 3. Example of estimated coefficients of elastic net under sampling uncertainty.

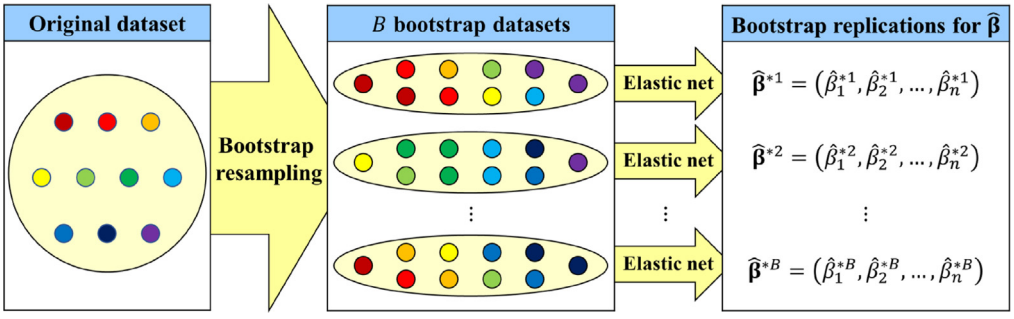

Fig. 4. Procedure for bootstrap resampling.

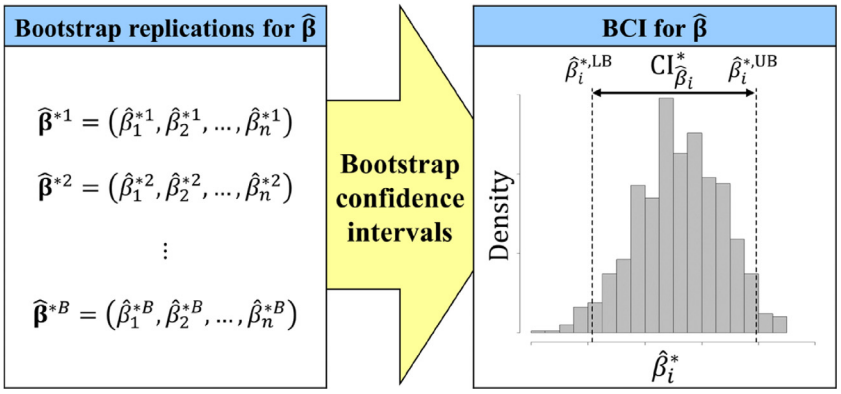

Fig. 5. Procedure for bootstrap confidence intervals.

function. When $\hat{z}_0 = 0$ and $\hat{a} = 0$, the BCIs are equal to that of using the percentile method. Parameter z_0 is defined as follows:

$$\hat{z}_0 = \Phi^{-1}\left(\frac{\#\left\{\hat{\beta}^*(b) < \hat{\beta}\right\}}{B}\right) \tag{4}$$

It is estimated by calculating the magnitude of bias, which is obtained from the proportion of the bootstrap replications less than $\hat{\beta}$, that is, $\hat{z}_0$ measures the median bias of $\hat{\beta}^*$, which is the discrepancy between the median of $\hat{\beta}^*$ and $\hat{\beta}$. Parameter a is estimated in terms of the skewness of the score function. Practically, to make the method general and not function-specific, the jackknife approximation method [31] was used to calculate $\hat{a}$ as follows:

$$\hat{a} = \frac{\sum_{i=1}^{N}\left(\hat{\beta}_{(-i)} - \hat{\beta}_{(\cdot)}\right)^3}{6\left\{\sum_{i=1}^{N}\left(\hat{\beta}_{(-i)} - \hat{\beta}_{(\cdot)}\right)^2\right\}^{3/2}}, \quad \hat{\beta}_{(\cdot)} = \frac{1}{N}\sum_{i=1}^{N}\hat{\beta}_{(-i)} \tag{5}$$

where $\hat{\beta}_{(-i)}$ is an estimate of β without the ith observed data point. In summary, the basic, bootstrap-t, and percentile methods are appropriate for estimating the parameters of interests under certain circumstances. However, when a parameter is a function of the parameters of interest, it is difficult to estimate the standard deviation, and the bootstrap distribution is biased and skewed. The methods estimate confidence intervals significantly different from the true values. Therefore, this study used the BCa method to calculate the BCIs for the estimated coefficients.

3. RENBOOT

This study proposes a robust elastic net via the bootstrap method (RENBOOT) to analyze the significance of input variables by reducing sampling uncertainty (see Fig. 6). First, B bootstrap datasets are resampled using balanced bootstrap resampling for the original dataset. Second, the coefficients of the elastic net are estimated for each bootstrap dataset. Third, the BCIs for the estimated coefficients are calculated using the BCa method. Fourth, the relevance of the input variables is analyzed using the statistical criterion. Finally, the significances of relevant input variables are analyzed using the significance measure.

3.1. Relevance of input variables using statistical criterion

Screening of irrelevant input variables is necessary to accurately analyze the significances of input variables. This study uses the following statistical criterion [29] based on BCIs:

$$r_i = \begin{cases} 1, & \text{if } 0 \notin \mathrm{CI}^*_{\hat{\beta}_i} \\ 0, & \text{otherwise} \end{cases} \qquad \mathrm{CI}^*_{\hat{\beta}_i} = \left[\hat{\beta}_i^{*,\mathrm{LB}},\ \hat{\beta}_i^{*,\mathrm{UB}}\right] \tag{6}$$

where $\mathrm{CI}^*_{\hat{\beta}_i}$ is the BCI for the estimated coefficient of the ith input variable; r_i is the relevance of the ith input variable; $\hat{\beta}_i^{*,\mathrm{LB}}$ and $\hat{\beta}_i^{*,\mathrm{UB}}$ are the lower and upper bounds of the BCI for $\hat{\beta}_i$, respectively. If the ith input variable has nonzero overlapping $\mathrm{CI}^*_{\hat{\beta}_i}$, r_i is 1. This means that the ith input variable is relevant to a response. Otherwise, r_i is 0, which means that the ith input variable is irrelevant to the response.

The statistical criterion is similar to the criterion for analyzing the relevance of the elastic net, but there exists a difference. The elastic net analyzes relevance based on the estimated coefficients. In contrast, as the statistical criterion analyzes relevance based on the BCIs, it is possible to analyze the relevance of input variables by reducing sampling uncertainty.

3.2. Significance of input variables using significance measure

The importance measure [30] using the bootstrap replications for $\hat{\beta}_i$ and the BCIs for $\hat{\beta}_i$ was proposed as follows:

$$\mathrm{Imp}_i = \frac{\left|\mathrm{mean}\left(\hat{\boldsymbol{\beta}}_i^*\right)\right|}{\left(\hat{\beta}_i^{*,\mathrm{UB}} - \hat{\beta}_i^{*,\mathrm{LB}}\right)^2} \tag{7}$$

where Imp_i is the importance (significance) of the ith input variable and $\hat{\boldsymbol{\beta}}_i^*$ is the bootstrap replications for $\hat{\beta}_i$. The higher the absolute value of the mean of $\hat{\boldsymbol{\beta}}_i^*$, the higher the significance. Moreover, as the difference between the upper and lower bounds of the BCIs for $\hat{\beta}_i$ decreases, the significance increases.

There are four cases in which the significance of x_1 and x_2 are analyzed differently (assume that there are only two input variables), and listed in Table 1.

Graphical representations of Table 1 are shown in Fig. 7. As shown in Fig. 7(a) , since x_2 has a higher mean and shorter length of BCIs than x_1, we can analyze that x_2 has a higher significance. As shown in Fig. 7(b), the length of BCIs of x_1 and x_2 are similar, but since the mean of x_2 is higher, it can be analyzed that the significance of x_2 is high. In Fig. 7(c) and (d), the significance of x_1 can be analyzed higher than x_2 due to the length of BCIs. Certainly, if the mean is similar as shown in Fig. 7(d), it is reasonable to analyze that the significance of x_1 is higher than x_2. However, in Fig. 7(c), although the magnitude of the estimated coefficients of x_2 is higher than x_1, it is unclear whether it is correct to analyze that the significance of x_1 is higher due to the denominator term (the length of BCIs). Additionally, when the length of BCIs in the denominator term is very small, its significance can fluctuate sensitively. In other words, this study analyzed that there was an issue in the robustness of significance by the length of BCIs in Eq. (7).

Table 1
Four cases where x_1 and x_2 have different significances.

	$\left\|\mathrm{mean}\left(\hat{\boldsymbol{\beta}}_i^*\right)\right\|$	$\hat{\beta}_i^{*,\mathrm{UB}} - \hat{\beta}_i^{*,\mathrm{LB}}$
Case 1	$x_1 < x_2$ $(x_1 > x_2)$	$x_1 > x_2$ $(x_1 < x_2)$
Case 2	$x_1 < x_2$ $(x_1 > x_2)$	$x_1 \cong x_2$
Case 3	$x_1 < x_2$ $(x_1 > x_2)$	$x_1 < x_2$ $(x_1 > x_2)$
Case 4	$x_1 \cong x_2$	$x_1 < x_2$ $(x_1 > x_2)$

It is certain that the length of BCIs can provide useful information about whether they are statistically confident to analyze significance, but formulating them into the denominator term like Eq. (7) can be a problem. Therefore, this study used BCIs to determine whether the input variable was relevant or irrelevant, and used the mean, which is a simple but robust significance measure as follows:

$$s_i = \left|\mathrm{mean}\left(\hat{\boldsymbol{\beta}}_i^*\right)\right| \tag{8}$$

where s_i is the significance of the ith input variable. The significance measure can robustly obtain the significance by removing the denominator of the importance measure. Furthermore, variations in $\hat{\beta}_i$ caused by the sampling uncertainty can be reduced owing to the bootstrap replication for $\hat{\beta}_i$. Because the significance measure does not use BCIs previously used in the relevance analysis, information loss occurs. Further studies on new significance measure to correctly analyze the significance based on BCIs in different ways are required.

3.3. Comparison between elastic net and RENBOOT using mathematical examples

The elastic net and RENBOOT were compared to identify the reduction of the sampling uncertainty through the mathematical examples. To reflect the sampling uncertainty, 100 different datasets were sampled using OLHD. The balanced accuracy (BA) [36], F1 score (F_1) [37], and Cohen's kappa (κ) [38] were used to evaluate how accurately the relevant input variables and irrelevant input variables were analyzed.

$$\mathrm{BA} = \frac{1}{2}\left(\frac{TP}{TP+FN} + \frac{TN}{FP+TN}\right) \times 100\ [\%] \tag{9}$$

$$P = \frac{TP}{TP+FP} \tag{10}$$

$$R = \frac{TP}{TP+FN} \tag{11}$$

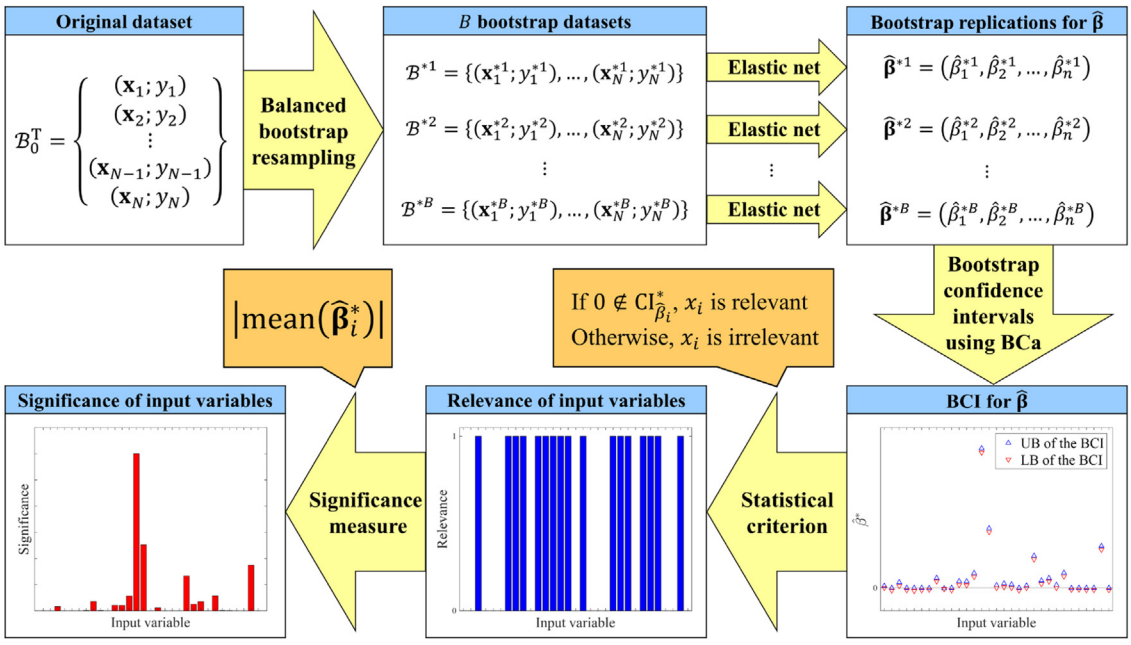

Fig. 6. Procedure of RENBOOT.

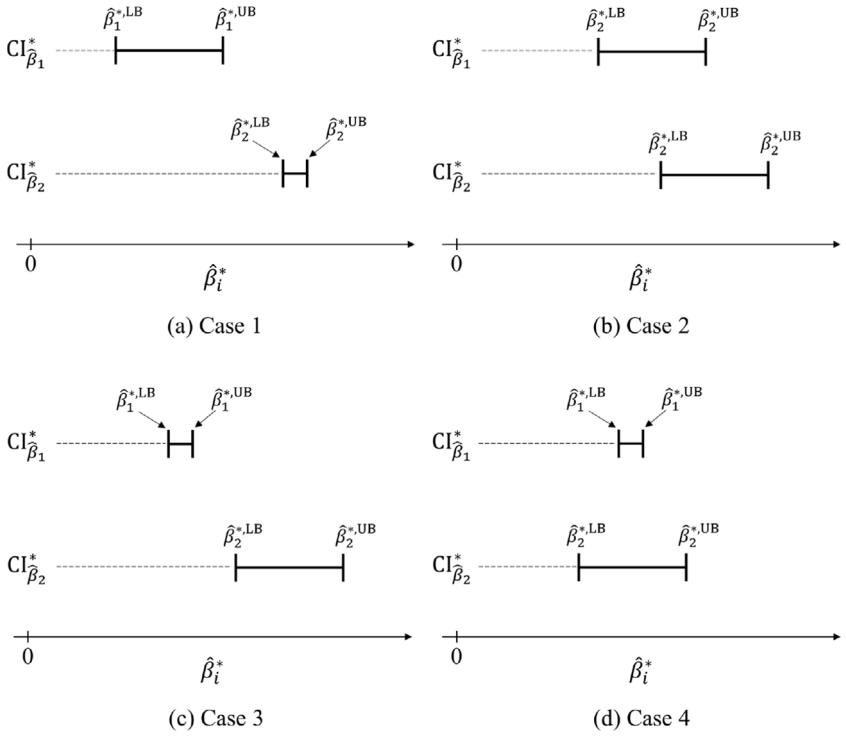

Fig. 7. Graphical representations of the four cases where x_1 and x_2 have different significances.

$$F_1 = 2\frac{P \cdot R}{P + R} \times 100 \ [\%] \tag{12}$$

$$P_0 = \frac{TP + TN}{TP + TN + FP + FN} \tag{13}$$

$$P_1 = \frac{TP + FN}{TP + TN + FP + FN} \tag{14}$$

$$P_2 = \frac{TP + FP}{TP + TN + FP + FN} \tag{15}$$

$$P_e = P_1 P_2 + (1 - P_1)(1 - P_2) = \frac{(TP + FN)(TP + FP) + (TN + FP)(TN + FN)}{(TP + TN + FP + FN)^2} \tag{16}$$

$$\kappa = \frac{P_0 - P_e}{1 - P_e} \times 100 \ [\%] \tag{17}$$

Each term of Eq. (9) is demonstrated in Table 2. The first and second terms in Eq. (9) are, respectively, the ratios of accurately estimated relevant and irrelevant input variables. When the ratio of *TP* to *TN* increases, BA increases, which implies that the accuracy of analyzing the relevant and irrelevant input variables is high. Precision (P) is the ratio of true positive among the

Table 2
Confusion matrix for relevant and irrelevant input variables.

Estimated	True	
	Relevant input variable	Irrelevant input variable
Relevant input variable	True positive (*TP*)	False positive (*FP*)
Irrelevant input variable	False negative (*FN*)	True negative (*TN*)

model estimated as positive, and the recall (R) is the ratio of the model estimated as true positive among the true. F_1 is the harmonic mean of the precision and recall. It implies that if either the precision or recall is a low value, F_1 is evaluated to be very small. In other words, as both the precision and recall are higher, F_1 increases, and it is evaluated that the relevant input variables have been correctly analyzed. Observed accuracy (P_0) is calculated by the sum of the correctly analyzed numbers divided by the total numbers. Expected accuracy (P_e) is the probability expected by chance. That is, as the overall accuracy is higher and the expected accuracy is lower, κ increases, and it is evaluated that the relevance of input variables are correctly analyzed.

The root mean square error (RMSE), expressed in Eq. (18), was used to evaluate how accurately the significance of input variables was analyzed.

$$\mathrm{RMSE}_i = \sqrt{\frac{1}{R}\sum_{r=1}^{R}\left(\widehat{\mathrm{ranking}}_{i,r} - \mathrm{ranking}_i\right)^2} \tag{18}$$

In Eq. (18), $\mathrm{ranking}_i$ is the true ranking of the significance of the ith input variable, $\widehat{\mathrm{ranking}}_{i,r}$ is the estimated ranking of the significance of the ith input variable for the rth dataset, R is the number of datasets, and RMSE_i is the RMSE of the ith input variable. For all datasets, the smaller the difference between the true and estimated rankings of each input variable, the smaller the RMSE, which indicates that the accuracy of analyzing the significance is high.

The first mathematical example was formulated to validate the relevance and significance of input variables in the low-dimensional problem similar to Fig. 3.

$$\begin{aligned} y_0 &= \sum_{i=1}^{4} f_i(x_i) \\ f_1(x) &= x \\ f_2(x) &= 0.3 \\ f_3(x) &= 0.7 \\ f_4(x) &= 0.8(x-1)^2 + 0.1 \end{aligned} \tag{19}$$

In this example, the number of input variables is 4, and the impact of input variables on y_0 within the design domain is depicted in Fig. 8. The relevant input variables are x_1 and x_4, and the irrelevant input variables are x_2 and x_3. The ranking of the significance of input variables is x_1, x_4, and $x_2 = x_3$.

Based on Eq. (20), the number of data points for y_0 was composed of 15.

$$N = \frac{(n+1)(n+2)}{2} \tag{20}$$

The BA of y_0 of elastic net and RENBOOT were 85.50% and 99.50%, respectively. And, the F_1 of y_0 of elastic net and RENBOOT were 87.34% and 99.50%, respectively. Finally, the κ of y_0 of elastic net and RENBOOT were 71.00% and 99.00%, respectively. Particularly, the irrelevant input variables, x_2 and x_3, were analyzed as relevant input variables using the elastic net in many cases. In other words, the coefficients of x_2 and x_3 should be analyzed to be exactly 0, but there were cases where they had values depending

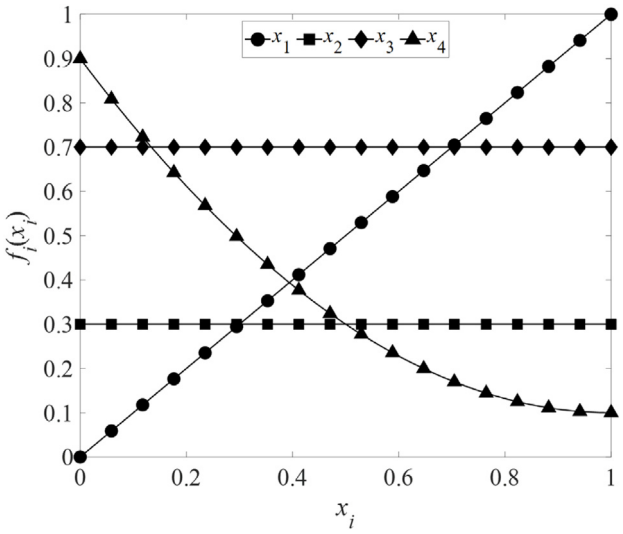

Fig. 8. Impact of input variables on y_0.

on the datasets. Additionally, the RMSE of y_0 of elastic net for x_1, x_2, x_3, x_4 were 0.0000, 0.4796, 0.4899, and 0.0000. And, the RMSE of y_0 of RENBOOT for x_1, x_2, x_3, x_4 were 0.1000, 0.1000, 0.1414, and 0.1000. In particular, the RMSE of RENBOOT for irrelevant input variables (x_2, x_3) was considerably lower than that of the elastic net. For this low-dimensional problem, the accuracies of the relevance and significance of input variables using RENBOOT were highly improved when compared with those of the elastic net.

The second mathematical example was formulated to validate the relevance and significance of input variables in the high-dimensional problem.

$$\begin{aligned} y_1 &= \sum_{i=1}^{15} f_i(x_i) \\ f_1(x) &= x \\ f_2(x) &= -0.9x^2 + 1 \\ f_3(x) &= -0.8x + 0.85 \\ f_4(x) &= -0.7(x-1)^2 + 0.85 \\ f_5(x) &= 0.6x + 0.3 \\ f_6(x) &= 0.5(x-1)^2 + 0.3 \\ f_7(x) &= -0.4x + 0.55 \\ f_8(x) &= 0.3x^2 + 0.45 \\ f_9(x) &= 0.2x + 0.6 \\ f_{10}(x) &= -0.1x^2 + 0.6 \\ f_{11}(x) &= 0 \\ f_{12}(x) &= 0.25 \\ f_{13}(x) &= 0.5 \\ f_{14}(x) &= 0.75 \\ f_{15}(x) &= 1 \end{aligned} \tag{21}$$

In this example, the number of input variables is 15, and the impact of input variables on y_1 within the design domain is depicted in Fig. 9. The relevant input variables are $x_1, x_2, \ldots, x_{10}$ and the irrelevant input variables are $x_{11}, x_{12}, \ldots, x_{15}$. The significance of input variables was configured to decrease from x_1

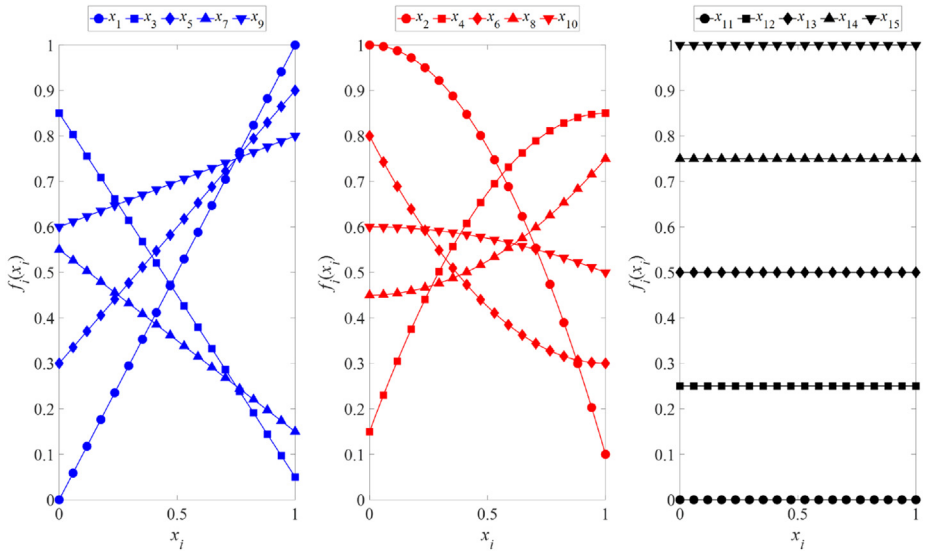

Fig. 9. Impact of input variables on y_1.

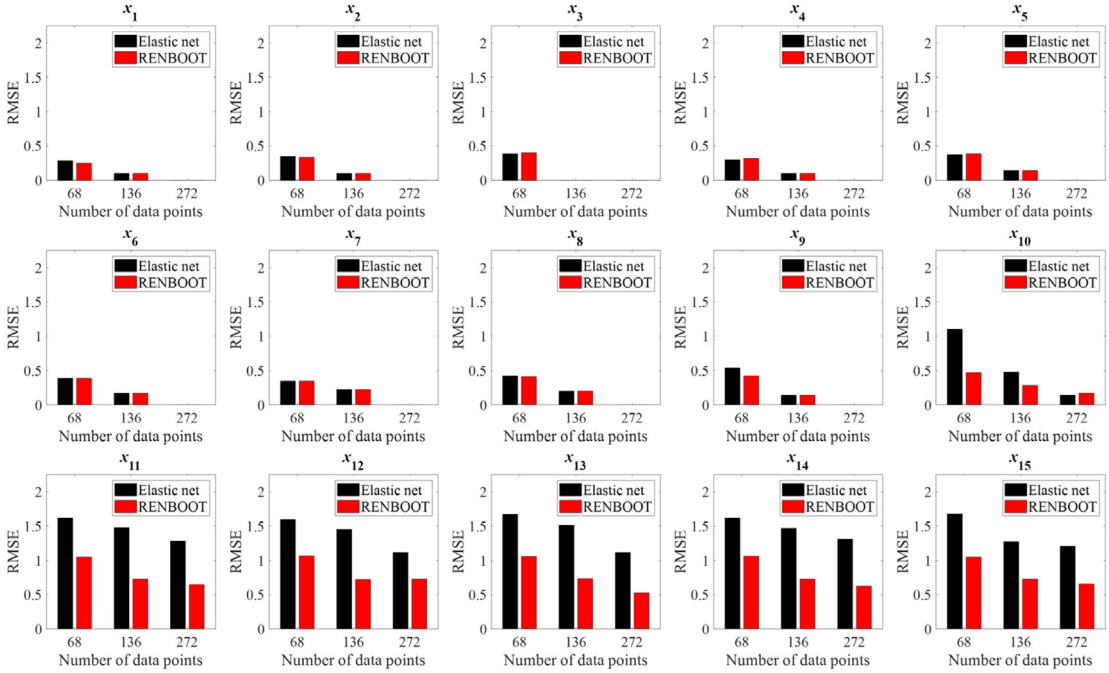

Fig. 10. Root mean square error of y_1.

to x_{10}. x_1, x_3, x_5, x_7, x_9 were configured to have linear response characteristics, and $x_2, x_4, x_6, x_8, x_{10}$ were configured to have nonlinear response characteristics of the degree of a second order polynomial. That is, y_1 is configured to reflect the various effects of input variables.

Additionally, y_2 was formulated to analyze the significance of a response with the two-factor interaction term, as shown in Eq. (22):

$$y_2 = y_1 + x_1 x_5 \tag{22}$$

The two-factor interaction effect of y_2 analyzed via ANOVA was approximately 4.03%. Although the two-factor interaction effect is not high, it can be considered that the response characteristic of y_2 has some generality because the interaction effect of the general engineering design problem is not high [39]. To summarize, the rankings of the significances of input variables for y_1 and y_2 are listed in Table 3.

Table 3
Rankings of the significances of input variables for y_1 and y_2 in mathematical examples.

Response	x_1	x_2	x_3	x_4	x_5	x_6	x_7	x_8	x_9	x_{10}	x_{11}	x_{12}	x_{13}	x_{14}	x_{15}
y_1	1	2	3	4	5	6	7	8	9	10	11	11	11	11	11
y_2	1	3	4	5	2	6	7	8	9	10	11	11	11	11	11

Based on Eq. (20), the number of data points for y_1 and y_2 was composed of 136 (N), respectively. Additionally, the tendency of accuracy based on the number of data points $0.5N, N$, and $2N$ was identified for y_1 and y_2. The balanced accuracy, F1 score, and Cohen's kappa of y_1 and y_2 are described in Tables 4 and 5, respectively.

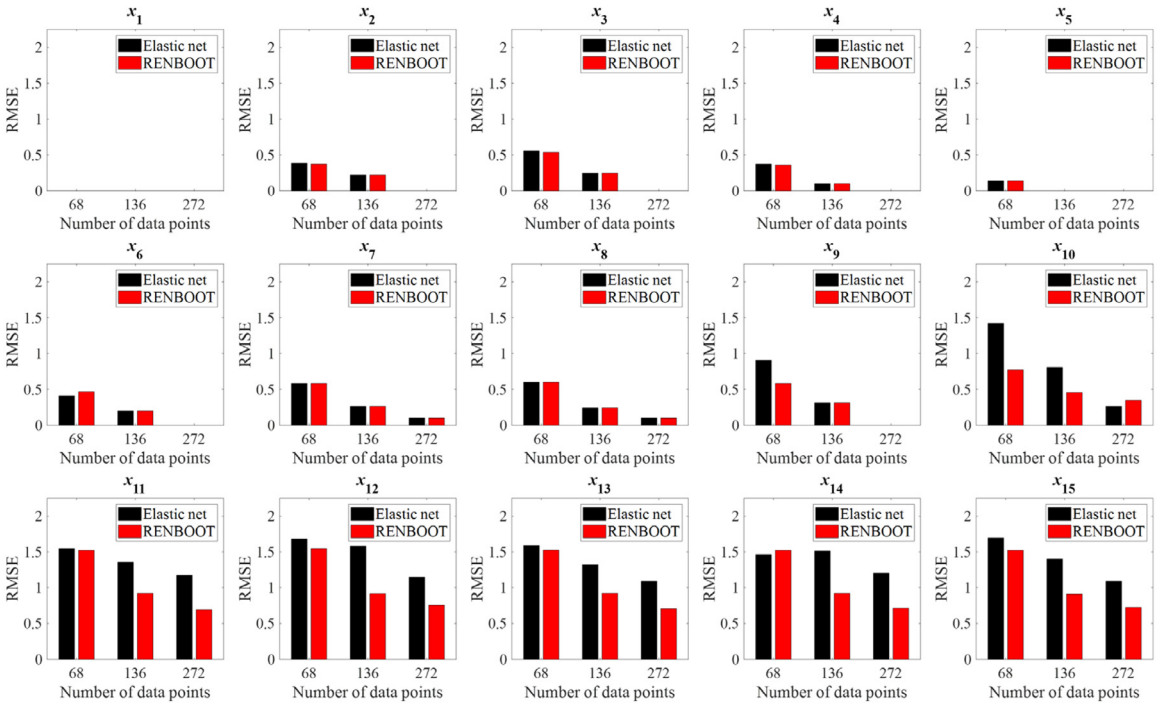

Fig. 11. Root mean square error of y_2.

Table 4
Balanced accuracy, F1 score, and Cohen's kappa of y_1.

Accuracy measure		BA [%]		F_1 [%]		κ [%]	
Method		Elastic net	RENBOOT	Elastic net	RENBOOT	Elastic net	RENBOOT
Number of data points	68	78.35	94.55	89.85	94.67	62.90	85.34
	136	84.30	96.25	92.66	96.62	74.32	90.33
	272	88.25	96.00	94.42	97.83	81.21	93.31

Table 5
Balanced accuracy, F1 score, and Cohen's kappa of y_2.

Accuracy measure		BA [%]		F_1 [%]		κ [%]	
Method		Elastic net	RENBOOT	Elastic net	RENBOOT	Elastic net	RENBOOT
Number of data points	68	78.35	92.65	89.37	92.27	62.07	79.79
	136	83.35	95.05	92.06	95.39	72.23	87.10
	272	89.00	94.45	94.73	96.19	82.41	88.63

For all cases, the accuracies of RENBOOT were improved when compared with those of the elastic net. Particularly, in the case of y_2, which has the two-factor interaction effects of x_1 and x_5, the accuracies of RENBOOT were higher than those of the elastic net. As the number of data points increases, the differences between the elastic net and RENBOOT decrease. However, because the sampling uncertainty is high when the number of data points is small, it can be seen that the differences between the elastic net and RENBOOT are large. From the point of view of the sampling uncertainty, the high improvements of RENBOOT are considered as a meaningful result.

The RMSE of y_1 is depicted in Fig. 10. In most cases, the RMSE of RENBOOT was less than that of the elastic net. For x_3, x_4, x_5, x_6, x_7, the RMSE of RENBOOT was similar to that of the elastic net or slightly higher. In particular, the RMSE of RENBOOT for low significance input variables (x_9, x_{10}) and irrelevant input variables $(x_{11}, x_{12}, \ldots, x_{15})$ was considerably lower than that of the elastic net. From the point of view of the significant input variable selection, RENBOOT can provide more useful information than the elastic net. Additionally, it is evident that the reduction in RMSE for $x_1, x_2, x_8, x_9, x_{10}, x_{15}$ is higher when the number of data points is small.

The RMSE of y_2 is depicted in Fig. 11. Similar to y_1, the RMSE of RENBOOT was less than that of the elastic net for most cases. For x_1, x_5, x_6, x_7, x_8, the RMSE of RENBOOT was similar to that of the elastic net or slightly higher. It is evident that the difference between the RMSE of the elastic net and RENBOOT was lower than that of y_1 owing to the increase in the nonlinear response characteristics. However, the RMSE of RENBOOT for low significance input variables (x_9, x_{10}) and irrelevant input variables $(x_{11}, x_{12}, \ldots, x_{15})$ were considerably decreased. Furthermore, the reduction in RMSE for $x_2, x_3, x_4, x_9, x_{10}$ was higher when the number of data points was small.

4. Application to the BIW of a vehicle

RENBOOT was applied to analyze the significance of input variables for the BIW of a vehicle [32]. The finite element (FE) model of the BIW of a vehicle was developed by the National Crash Analysis Center of the George Washington University. This study used the FE model, as depicted in Fig. 12, provided by LS-DYNA [32].

Fig. 12. BIW of a vehicle (left) and input variables (right) [40].

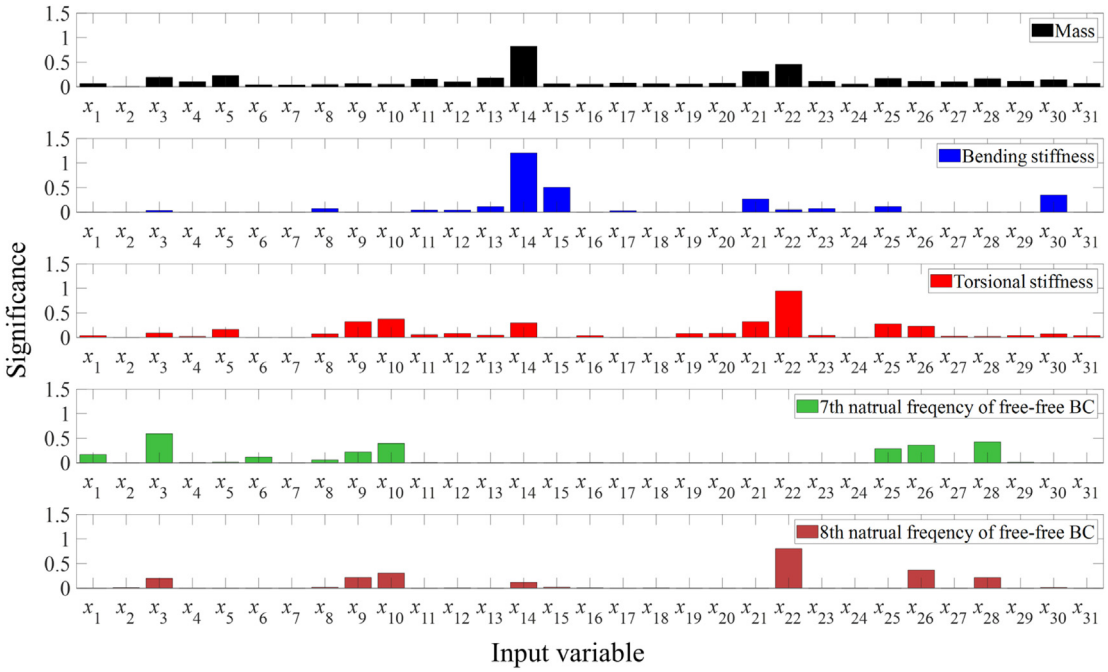

Fig. 13. Significances of input variables for the BIW.

The input variables were the sheet thickness (in mm), and the number of input variables was 31. The descriptions and design domains of the input variables are listed in Table 6.

The number of responses of the BIW of a vehicle was 5: mass, bending stiffness, torsional stiffness, and the 7th and 8th natural frequencies of the free–free boundary condition (BC). The details of the five responses are explained in Section 4.2 of our previous study [40]. Mass (in tons) was measured as the total body mass, shown on the left side in Fig. 13. The bending stiffness (in N/mm) was measured as the sum of the Z-directional loads divided by the Z-directional deformation. The loading and boundary conditions for the bending stiffness were set by referring to the SAE Technical Paper [41]. The torsional stiffness (in N·mm/deg) was measured as the X-directional moment divided by the torsional angle (YZ-plane). The loading and boundary conditions for the torsional stiffness were set by referring to Livermore Software Technology Corporation [32]. The 7th and 8th natural frequencies of the free–free BC [Hz] were measured by performing modal analysis. As the free–free BC was set, the natural frequencies of the 7th and 8th were measured without measuring the natural frequencies from the 1st to the 6th natural frequencies.

OLHD was used for the sampling data for RENBOOT. The number of data points was 529, which was the sum of the values calculated using Eq. (20) and the initial design data point. The significances of input variables for the BIW of a vehicle were analyzed using RENBOOT, as depicted in Fig. 13.

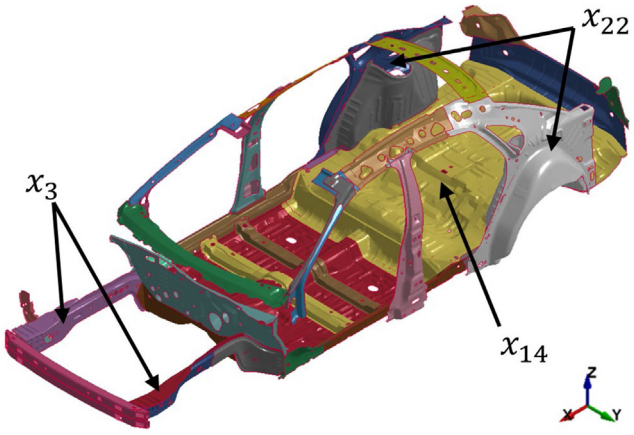

Fig. 14. Most significant input variable for each response of the BIW.

The ranking of the significances of the input variables for the mass was $x_{14}, x_{22}, x_{21}, x_5, x_3, \ldots, x_{10}, x_8, x_6, x_7, x_2$. The ranking of the significances of input variables for the bending stiffness was $x_{14}, x_{15}, x_{30}, x_{21}, x_{25}, \ldots, x_{22}, x_{11}, x_{12}, x_3, x_{17}$, and the other input variables were analyzed as irrelevant. The ranking of the significances of the input variables for the torsional stiffness was

Table 6
Descriptions and design domains of input variables for the BIW [40].

Input variable	Description	Initial design	Lower bound	Upper bound
x_1	Left and right rail plate 1	2.5100	2.0000	3.0000
x_2	Right rail plate 2	1.5200	1.0000	2.0000
x_3	Inner of left and right rail	1.9000	1.5000	2.5000
x_4	Outer of left and right rail	1.9100	1.5000	2.5000
x_5	Rear left and right rail	1.5000	1.0000	2.0000
x_6	Middle left and right reinforcement rail	2.5500	2.0000	3.0000
x_7	Middle left and right–left reinforcement rail 2	2.4000	2.0000	3.0000
x_8	Lower of left and right A-pillar 2	2.2000	1.5000	2.5000
x_9	Inner of left and right A-pillar	2.0000	1.5000	2.5000
x_{10}	Outer of left and right A-pillar	1.4000	1.0000	2.0000
x_{11}	Inner of left and right B-pillar	1.1000	0.7000	1.7000
x_{12}	Outer of left and right B-pillar	1.1500	0.7000	1.7000
x_{13}	Floor	0.8000	0.6000	1.0000
x_{14}	Rear floor	1.2000	0.7000	1.7000
x_{15}	Transverse reinforcement under floor	1.2000	0.7000	1.7000
x_{16}	Rear left and right floor extension	1.6500	1.0000	2.0000
x_{17}	Front cross member	1.2000	0.7000	1.7000
x_{18}	Rear cross member	1.4000	1.0000	2.0000
x_{19}	Rear transverse reinforcement roof	1.0000	0.7000	1.7000
x_{20}	Outer of left and right reinforcement roof	1.1000	0.7000	1.7000
x_{21}	Inner of rear left and right wheel well	0.9000	0.7000	1.7000
x_{22}	Outer of rear left and right wheel well	0.9000	0.7000	1.7000
x_{23}	Toe panel	1.9000	1.5000	2.5000
x_{24}	Left and right support reinforcement toe panel 1	2.5000	2.0000	3.0000
x_{25}	Firewall	0.7500	0.5000	1.0000
x_{26}	Inner of upper firewall	0.6500	0.6000	1.6000
x_{27}	Rear suspension frame	1.4000	1.0000	2.0000
x_{28}	Front bumper frame	1.2200	0.7500	1.7500
x_{29}	Outer of support trunk latch	0.7500	0.7000	1.7000
x_{30}	Inner of left and right rocker panel	1.2500	0.7000	1.7000
x_{31}	Rear left and right light mount	1.0000	0.7000	1.7000

$x_{22}, x_{10}, x_{21}, x_9, x_{14}, \ldots, x_{16}, x_1, x_{27}, x_4, x_{28}$, and the other input variables were analyzed as irrelevant. The ranking of the significances of the input variables for the 7th natural frequency of the free–free BC was $x_3, x_{28}, x_{10}, x_{26}, x_{25}, x_9, x_1, x_6, x_8$, and the other input variables were analyzed as irrelevant. Finally, the ranking of the significances of the input variables for the 8th natural frequency of the free–free BC was $x_{22}, x_{26}, x_{10}, x_9, x_{28}, x_3, x_{14}, x_{15}, x_8$, x_{30}, and the other input variables were analyzed as irrelevant.

The most significant input variable for each response is depicted in Fig. 14. First, x_{14} (rear floor) was analyzed as the most significant input variable for mass. Because x_{14} occupied the largest volume when compared with the other input variables, its significance analysis was considered appropriate. Second, x_{14} was analyzed as the most significant input variable for bending stiffness. Because Z-directional loads were applied to the seat bolting positions, x_{14}, which occupied a majority of the floor sheets, was analyzed as the largest significance. Third, x_{22} (outer of rear left and right wheel well) was analyzed as the most significant input variable for torsional stiffness. Because torsional moment was applied to the front shock towers, x_{22}, which is near the fixed rear shock towers, was analyzed as the largest significance. Fourth, x_3 (inner of left and right rail) was analyzed as the most significant input variable for the 7th natural frequency of free–free BC. Because the front portion was in a mode vibrating along the Y-direction, x_3 was analyzed as the largest significance. Finally, x_{22} was analyzed as the most significant input variable for the 8th natural frequency of free–free BC. Because the rear portion was in a mode vibrating along the Z-direction, x_{22} was analyzed as the largest significance.

5. Conclusions

The significance of input variables can be analyzed using the elastic net regardless of the data type of input variables and statistical assumptions. However, the accuracies of the relevance and significance of input variables using the elastic net fluctuate owing to the sampling uncertainty. This leads to incorrect inferences. Therefore, to reduce sampling uncertainty, RENBOOT using the bootstrap method for the elastic net was proposed. The major results of this study are summarized as follows:

- Sampling uncertainty of the elastic net is addressed
- RENBOOT is proposed to reduce the sampling uncertainty
- Statistical criterion and significance measure are used to analyze significance
- Accuracies of RENBOOT are significantly improved compared with those of elastic net
- Significance of input variables for the body-in-white of a vehicle is analyzed

The elastic net and RENBOOT were compared using mathematical examples. The BA, F_1, κ, and RMSE were calculated to compare the accuracies of the relevance and significance of the input variables. In most cases, the BA, F_1, κ, and RMSE of RENBOOT were superior to those of the elastic net. Particularly, the accuracies of RENBOOT for low significance input variables and irrelevant input variables were highly improved. From the point of view of the significant input variable selection, removing irrelevant input variables and selecting significant input variables are important. When compared with the elastic net, RENBOOT can provide more useful information for performing significant input variable selection. The difference in accuracies between the elastic net and RENBOOT is significant when the number of data points is small. In other words, the improvements afforded by RENBOOT increase as the number of data points decreases. Because sampling uncertainty is high when the number of data points is small, a significant improvement in accuracy is desirable. However, when the nonlinearity of a response increases, such as through the addition of interaction terms, the improvement in accuracy afforded by RENBOOT decreases slightly, as compared with the case without the interaction term. Thus, follow-up studies are necessary to improve the accuracy of RENBOOT when the nonlinearity of the response is high.

Furthermore, RENBOOT was used to analyze the significance of the input variables for the BIW of a vehicle. The significance was reasonably analyzed by considering the physical relationships from the most significant input variables to the irrelevant input variables. When significant input variable selection is performed based on significance, design optimization can be performed efficiently. The computational costs of RENBOOT are at least B times more than that of the elastic net when using bootstrap resampling. However, in high-dimensional, computationally expensive, black-box problems, where the computational costs for obtaining data points are significantly high, the computational costs required to perform RENBOOT are insignificant. As the computational costs of the bootstrap method are low, as compared with the computational costs for obtaining data, it is considered more effective to use RENBOOT by reducing the sampling uncertainty.

CRediT authorship contribution statement

Hansu Kim: Conceptualization, Methodology, Software, Validation, Writing - original draft, Writing - review & editing, Visualization. **Tae Hee Lee:** Conceptualization, Methodology, Writing - review & editing, Supervision, Project administration, Funding acquisition.

Declaration of competing interest

The authors declare that they have no known competing financial interests or personal relationships that could have appeared to influence the work reported in this paper.

Acknowledgments

The authors greatly appreciate the reviewers' comments and suggestions on improving this paper. This work was supported by the National Research Foundation of Korea (NRF), South Korea grant funded by the Korea government (MSIT) (No. NRF-2019R1A2C1007644).

References

[1] S.Q. Shan, G.G. Wang, Survey of modeling and optimization strategies to solve high-dimensional design problems with computationally-expensive black-box functions, Struct. Multidiscip. Optim. 41 (2) (2010) 219–241, http://dx.doi.org/10.1007/s00158-009-0420-2.

[2] R.E. Bellman, Dynamic Programming, first ed., Princeton University Press, Princeton, 1957.

[3] P.N. Koch, T.W. Simpson, J.K. Allen, F. Mistree, Statistical approximations for multidisciplinary design optimization: The problem of size, J. Aircr. 36 (1) (1999) 275–286, http://dx.doi.org/10.2514/2.2435.

[4] F. Capitanescu, A. Ahmadi, E. Benetto, A. Marvuglia, L. Tiruta-Barna, Some efficient approaches for multi-objective constrained optimization of computationally expensive black-box model problems, Comput. Chem. Eng. 82 (2015) 228–239, http://dx.doi.org/10.1016/j.compchemeng.2015.07.013.

[5] P. Pandita, I. Bilionis, J. Panchal, Extending expected improvement for high-dimensional stochastic optimization of expensive black-box functions, J. Mech. Des. 138 (11) (2016) 111412, http://dx.doi.org/10.1115/1.4034104.

[6] X.W. Cai, H.B. Qiu, L. Gao, X.Y. Shao, Adaptive radial-basis-function-based multifidelity metamodeling for expensive black-box problems, AIAA J. 55 (7) (2017) 2424–2436, http://dx.doi.org/10.2514/1.J055649.

[7] Y.H. Li, Y.Z. Wu, J.J. Zhao, L.P. Chen, A Kriging-based constrained global optimization algorithm for expensive black-box functions with infeasible initial points, J. Global Optim. 67 (1–2) (2017) 343–366, http://dx.doi.org/10.1007/s10898-016-0455-z.

[8] G.H. Cheng, T. Gjernes, G.G. Wang, An adaptive aggregation-based approach for expensively constrained black-box optimization problems, J. Mech. Des. 140 (9) (2018) 091402, http://dx.doi.org/10.1115/1.4040485.

[9] I.B. Chung, D. Park, D.H. Choi, Surrogate-based global optimization using an adaptive switching infill sampling criterion for expensive black-box functions, Struct. Multidiscip. Optim. 57 (4) (2018) 1443–1459, http://dx.doi.org/10.1007/s00158-018-1942-2.

[10] A. Saad, Z.M. Dong, B. Buckham, C. Crawford, A. Younis, M. Karimi, A new Kriging-Bat algorithm for solving computationally expensive black-box global optimization problems, Eng. Optimiz. 51 (2) (2019) 265–285, http://dx.doi.org/10.1080/0305215X.2018.1461853.

[11] R.H. Shi, L. Liu, T. Long, Y.F. Wu, Y.F. Tang, Filter-based adaptive Kriging method for black-box optimization problems with expensive objective and constraints, Comput. Methods Appl. Mech. Engrg. 347 (2019) 782–805, http://dx.doi.org/10.1016/j.cma.2018.12.026.

[12] L.M. Chen, H.B. Qiu, L. Gao, C. Jiang, Z. Yang, Optimization of expensive black-box problems via Gradient-enhanced Kriging, Comput. Methods Appl. Mech. Engrg. 362 (2020) 112861, http://dx.doi.org/10.1016/j.cma.2020.112861.

[13] F. Li, W.M. Shen, X.W. Cai, L. Gao, G.G. Wang, A fast surrogate-assisted particle swarm optimization algorithm for computationally expensive problems, Appl. Soft. Comput. 92 (2020) 106303, http://dx.doi.org/10.1016/j.asoc.2020.106303.

[14] K.J. Craig, N. Stander, D.A. Dooge, S. Varadappa, Automotive crashworthiness design using response surface-based variable screening and optimization, Eng. Comput. 22 (1–2) (2005) 38–61, http://dx.doi.org/10.1108/02644400510572406.

[15] H. Cho, S. Bae, K.K. Choi, D. Lamb, R.J. Yang, An efficient variable screening method for effective surrogate models for reliability-based design optimization, Struct. Multidiscip. Optim. 50 (5) (2014) 717–738, http://dx.doi.org/10.1007/s00158-014-1096-9.

[16] H. Kim, S. Kim, T. Kim, T.H. Lee, N. Ryu, K. Kwon, S. Min, Efficient design optimization of complex system through an integrated interface using symbolic computation, Adv. Eng. Softw. 126 (2018) 34–45, http://dx.doi.org/10.1016/j.advengsoft.2018.09.006.

[17] A. Spagnol, R. Le Rodolphe, S. Da Veiga, Global sensitivity analysis for optimization with variable selection, SIAM-ASA J. Uncertain. Quantif. 7 (2) (2019) 417–443, http://dx.doi.org/10.1137/18M1167978.

[18] H. Kim, T.H. Lee, Y. Song, K. Huh, Robust design optimisation of adaptive cruise controller considering uncertainties of vehicle parameters and occupants, Veh. Syst. Dyn. 58 (6) (2020) 987–1005, http://dx.doi.org/10.1080/00423114.2019.1627375.

[19] P.J. Ross, Taguchi Techniques for Quality Engineering: Loss Function, Orthogonal Experiments, Parameters and Tolerance Design, second ed., McGraw-Hill, New York, 1996.

[20] R.A. Fisher, Statistical Methods for Research Workers, eleventh ed., Oliver & Boyd, Edinburgh, 1950.

[21] H. Zou, T. Hastie, Regularization and variable selection via the elastic net, J. R. Stat. Soc. Ser. B Stat. Methodol. 67 (2005) 301–320, http://dx.doi.org/10.1111/j.1467-9868.2005.00503.x.

[22] M.D. McKay, R.J. Beckman, W.J. Conover, A comparison of three methods for selecting values of input variables in the analysis of output from a computer code, Technometrics 21 (2) (1979) 239–245, http://dx.doi.org/10.2307/1268522.

[23] M.E. Johnson, L.M. Moore, D. Ylvisaker, Minimax and maximin distance designs, J. Statist. Plann. Inference 26 (2) (1990) 131–148, http://dx.doi.org/10.1016/0378-3758(90)90122-B.

[24] L. Sun, J.C. Xu, Y. Tian, Feature selection using rough entropy-based uncertainty measures in incomplete decision systems, Knowledge-Based Syst. 36 (2012) 206–216, http://dx.doi.org/10.1016/j.knosys.2012.06.010.

[25] L. Wei, F.F. Wu, A.H. Wu, Weighted discriminative sparsity preserving embedding for face recognition, Knowledge-Based Syst. 57 (2014) 136–145, http://dx.doi.org/10.1016/j.knosys.2013.12.016.

[26] K. Qi, H. Yang, Q.Y. Hu, D.J. Yang, A new adaptive weighted imbalanced data classifier via improved support vector machines with high-dimension nature, Knowledge-Based Syst. 185 (2019) 104933, http://dx.doi.org/10.1016/j.knosys.2019.104933.

[27] I.G. Lee, Q.Q. Zhang, S.W. Yoon, D. Won, A mixed integer linear programming support vector machine for cost-effective feature selection, Knowledge-Based Syst. 203 (2020) 106145, http://dx.doi.org/10.1016/j.knosys.2020.106145.

[28] S. Klau, M.L. Martin-Magniette, A.L. Boulesteix, S. Hoffmann, Sampling uncertainty versus method uncertainty: A general framework with application to omics biomarker selection, Biom. J. 62 (3) (2020) 670–687, http://dx.doi.org/10.1002/bimj.201800309.

[29] A. Gorostiaga, J.L. Rojo-Álvarez, On the use of conventional and statistical-learning techniques for the analysis of PISA results in Spain, Neurocomputing 171 (2016) 625–637, http://dx.doi.org/10.1016/j.neucom.2015.07.001.

[30] S. Muñoz Romero, A. Gorostiaga, C. Soguero-Ruiz, I. Mora-Jiménez, J.L. Rojo-Álvarez, Informative variable identifier: Expanding interpretability in feature selection, Pattern Recognit. 98 (2020) 107077, http://dx.doi.org/10.1016/j.patcog.2019.107077.

[31] B. Efron, R.J. Tibshirani, An Introduction to the Bootstrap, first ed., Chapman & Hall/CRC, New York, 1994.

[32] LSTC, Full vehicle MDO, 2011, https://www.lsoptsupport.com/examples/optimization/full-vehicle-mdo/. (Accessed 19 March 2021).

[33] A.C. Davison, D.V. Hinkley, E. Schechtman, Efficient bootstrap simulation, Biometrika 73 (3) (1986) 555–566, http://dx.doi.org/10.2307/2336519.
[34] T.J. DiCiccio, B. Efron, Bootstrap confidence intervals, Stat. Sci. 11 (3) (1996) 189–228, http://dx.doi.org/10.1214/ss/1032280214.
[35] B. Efron, Better bootstrap confidence intervals, J. Amer. Statist. Assoc. 82 (397) (1987) 171–185, http://dx.doi.org/10.2307/2289144.
[36] J.P. Mower, PREP-Mt: predictive RNA editor for plant mitochondrial genes, BMC Bioinformatics 6 (2005) 96, http://dx.doi.org/10.1186/1471-2105-6-96.
[37] Y. Sasaki, The Truth of the F-Measure, School of Computer Science, M1 7DN, University of Manchester MIB, 2007.
[38] J. Cohen, A coefficient of agreement for nominal scales, Educ. Psychol. Meas. 20 (1) (1960) 37–46, http://dx.doi.org/10.1177/001316446002000104.
[39] J. Antony, D. Preece, Understanding, Managing and Implementing Quality: Frameworks, Techniques, and Cases, first ed., Psychology Press, New York, 2002.
[40] H. Kim, T.H. Lee, T. Kwon, Normalized neighborhood component feature selection and feasible-improved weight allocation for input variable selection, Knowl.-Based Syst. 218 (2021) 106855, http://dx.doi.org/10.1016/j.knosys.2021.106855.
[41] J. Deleener, P. Mas, L. Cremers, J. Poland, Extraction of static car body stiffness from dynamic measurements. SAE Technical Paper 2010-01-0228, 2010, http://dx.doi.org/10.4271/2010-01-0228.